A313

Temporal Evolution of Low-Frequency Seismicity Preceding the 13 February 2014 Plinian Eruption at Kelud Volcano

〇Vico L. IPMAWAN, Masato IGUCHI, Haruhisa NAKAMICHI

Kelud Volcano, East Java, Indonesia, erupted on 13 February 2014 in a Plinian style with a Volcanic Explosivity Index (VEI) of 4, producing an ash column reaching up to 17 km in height. Volcanic ash from the eruption was dispersed as far as 530 km westward and up to 90 km northeastward. As one of the most recent monitored Plinian eruptions, the 2014 Kelud eruption provides an important case study for examining precursory processes leading to Plinian eruptions. This study aims to investigate precursory characteristics associated with Plinian eruptions and to discuss the broader implications of these findings for forecasting future large-scale explosive eruptions at other volcanoes, such as Sakurajima.

The 2014 Plinian eruption was preceded by several precursory phenomena. Increased gas emissions were first observed in December 2013, followed by the appearance of gas emissions around the margins of the lava dome in early February. Inflation recorded by strainmeters was detected in early December 2013 and showed accelerated deformation on 13 February, the same day as the Plinian eruption. Seismicity increased significantly in January, marked by the emergence of volcano-tectonic (VT) earthquakes, followed by the appearance of low-frequency (LF) earthquakes in early February 2014. This marked increase in seismicity was accompanied by enhanced thermal energy around the crater, with a temperature increase of approximately 4 °C detected on 22 January 2014.

Following the escalation of volcanic activity, an evacuation order was issued by the Center for Volcanology and Geological Hazard Mitigation (CVGHM) at 21:15 local time on 13 February 2014. Lava dome destruction occurred at 22:46, followed by the onset of the Plinian eruption at 23:01 local time.

Seismicity immediately prior to the eruption became extremely dense, resulting in the overlap of different earthquake signals that appeared as merged waveforms and evolved into continuous tremor-like signals. Therefore, in addition to classifying seismic events into VT and LF types, seismic energy partitioning was performed based on low-frequency (LF; 2.5–4.5 Hz) and high-frequency (HF; 6.5–13.5 Hz) bands (Figure 1). Subsequently, LF seismic energy was used as input for the Failure Forecast Method (FFM), as LF seismicity commonly appears as a precursor to large-scale eruptions, such as those observed at Pinatubo in 1991 and Sakurajima in 1914. The output of the FFM analysis provides an estimate of eruption timing.

The cumulative partitioned seismic energy curves show different acceleration onset times. HF seismic energy began accelerating on 9 February 2014, whereas LF energy showed acceleration on 13 February. The cumulative HF seismic energy reached 2.48×10^9 J, while the cumulative LF energy reached 7.56×10^8 J. Nevertheless, the energy density in the LF band was higher, particularly after 21:00 local time, indicating intensified seismic activity related to fluid movement or resonance processes prior to the Plinian eruption at Kelud.

To objectively identify optimal time windows for applying the FFM, deterministic algorithmic optimization based on dynamic programming was combined with Bayesian Information Criterion (BIC)–

based statistical model selection. Four FFM application periods were identified: Period 1 from 12 January 2014 at 00:10 to 8 February 2014 at 17:10; Period 2 from 8 February 2014 at 17:20 to 11 February 2014 at 14:20; Period 3 from 11 February 2014 at 14:30 to 12 February 2014 at 21:50; and Period 4 from 12 February 2014 at 22:00 to 13 February 2014 at 21:30. These four periods yielded eruption time predictions with lead times of 80 h 45 min, 49 h 24 min, 17 h 22 min, and 0 h 6 min relative to the actual eruption. The results demonstrate that FFM applications closer to the eruption onset systematically improve prediction accuracy, providing increasingly reliable lead times for hazard mitigation and evacuation decision-making.

A conceptual eruption process model based on the 2014 Kelud eruption was developed to extract generalizable features of Plinian eruption processes. The sequence can be described as follows: the early stage is characterized by a accelerated increase in VT seismicity accompanied by steep ground deformation, interpreted as rapid magma intrusion into the brittle zone that generates high-frequency seismicity. The subsequent stage is characterized by a rapid increase in LF seismicity, which is interpreted as reflecting increased volatile content and intensified gas exsolution activity. The late stage is characterized by rapid decompression, which serves as a prerequisite for accelerated gas release that ultimately triggers the Plinian eruption (Figure 1).

Based on the 2014 Kelud Plinian eruption, eruption timing can be constrained using the acceleration of cumulative partitioning LF seismic energy through the FFM, while a conceptual Plinian eruption process model can also be derived. Together, these outcomes demonstrate applicability to other volcanoes in forecasting future large-scale explosive eruptions, such as those at Sakurajima.

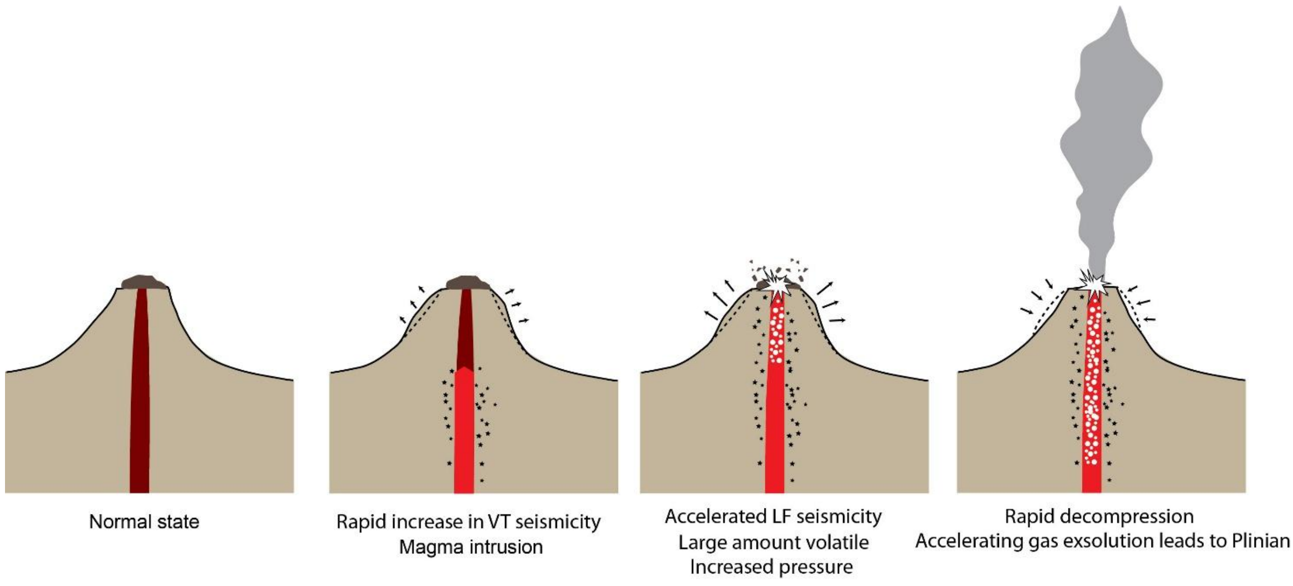

Figure 1. A conceptual Plinian eruption process model based on the 2014 Kelud eruption.